Migration Letters

Volume: 20, No: S9(2023), pp. 591-611

ISSN: 1741-8984 (Print) ISSN: 1741-8992 (Online)

www.migrationletters.com

Piezoelectric Energy Harvesting from Vortex-Induced Vibrations: Design and Correlations

Hadeer Abd UL-Qader Mohammed[1], Dr. Waleed Al-Ashtari[2]

Abstract

This study delves into the design optimization of a hydropower harvesting system, exploring various parameters and their influence on system performance. By modifying the variables within the model to suit different flow conditions, a judiciously optimized design is attainable. Notably, the lift force generated is found to be intricately linked to the strategic interplay of the bluff body's location, cylinder dimensions, and flow velocity. The findings culminate in the establishment of empirical equations, one for lift force and another for displacement, based on the force equation.

Many energy harvesting approaches hinge on the reciprocating motion inherent to the structural system. The methodology developed in this study emerges as a potent tool for generating optimal designs for such energy harvesting devices, contingent on the specified assumptions and constraints outlined in this paper.

The foundational steps in the design process commence with the formulation of modeling equations, contingent on four critical design parameters. This comprehensive model is implemented in ANSYS, yielding an optimized system configuration. Subsequently, the values representing the generated power for these optimal design parameters are ascertained.

The culmination of this research underscores that superior outcomes are achieved with a 0.5 D separation between the beam and cylinder, a cylinder diameter of 50 mm, and a flow velocity of 1.25 meters per second.

Keywords: *ANSYS, Piezoelectric Energy, hydropower.*

1. Introduction

The concept of harnessing energy from vortex-induced vibrations around a circular cylinder has undergone extensive investigation. Utilizing computational analysis and experimental work, we concurrently addressed the piezoelectric transducer, flow dynamics, and roller movement. The results reveal a significant correlation between cylinder placement, deflection of the piezoelectric energy harvester, vortex shedding, and captured power. It is evident that bringing the cylinder closer to the harvester expands the synchronization zone. As the energy output depends on vortex characteristics, frequency, and amplitude, studying different cylinder locations, fluid velocities, cylinder diameters, and beam geometries is crucial for optimal harvester design.

[1] Mechanical Engineering Department, Collage of Engineering, University of Baghdad, Jadriya, Baghdad, Iraq, h.mohammed1803d@coeng.uobaghdad.edu.iq

[2] Mechanical Engineering Department, Collage of Engineering, University of Baghdad, Jadriya, Baghdad, Iraq, Waleed.Al.Ashtari@coeng.uobaghdad.edu.iq

Piezoelectric polymer strips, often referred to as piezoelectric rods, were equipped with scour sensors for soil scanning. The sensor's structural dynamics and stimulating fluid velocity influence the voltage response. Monitoring both flow rate and shedding frequency enables the measurement of pressure rod exposure [1].

A mechanical solution is proposed by coupling cantilever piezoelectric vibration energy harvesters with inertial amplifiers. This technique can achieve significant inertial amplification orders under specific circumstances. Both broadband random excitation and harmonic excitation scenarios are considered, employing harvester circuits with and without inductors. We demonstrate how tuning different inertial amplifier parameters optimizes power collection under various excitations and circuit designs. When ambient excitation is aligned, the potential for harvesting five times the energy at 50% lower frequency is realized [2].

The introduction of an attraction magnet halts harvester ringing, establishing a nearly constant balanced state. The energy harvester's output is modeled using a distributed parameter model based on modal analysis. This model incorporates passive stiffness in higher mechanics, incorporating force-displacement data. At 9Hz and 3g of input acceleration, the highest RMS power reaches 1.20mW [3].

In MATLAB optimization research, model size, flow velocity, and resistance are explored as design parameters to determine the optimal range for energy extraction. Vortex-induced vibrations, resulting from the connection of a half-cylinder to a water-based beam, lead to piezoelectric deformation. The extended Hamiltonian principle of the cantilever (cylinder-like) beam, along with parametric equations based on the modified van der Pol model of the bluff body, elucidates the mechanical system [4 & 5].

The enhancement of the original PSMC agent-based sliding mode control, incorporating an AAC term of adaptive approximation compensator, simplifies stability proofing, accounting for non-model dynamics. Lyapunov's theorem systematically proves the stability of the proposed control method. Galperin's approach establishes the multimodal equation of motion. Simulation experiments were conducted using MATLAB/SIMULINK [6].

The nonlinear van der Pol equation encapsulates the flow-solid-electric coupling equations used to determine output voltage. The finite central difference approach enhances output performance and vibration responsiveness. Theoretical findings indicate that as water velocity decreases, vibration frequency, amplitude, and average power increase. Adjusting structural mass and load resistance to available water velocity further augments average collected power [7, 8].

Tests in a wind tunnel reveal that the energy harvester, when inserted into a formation of up to 25 cylinders, significantly amplifies power output through vortex interactions. Experiments demonstrate power production at the nano-watt level, highlighting the potential of formation effects in enhancing micro-scale wind energy harvesting [9].

The Lamb wave method proves effective for structural health monitoring using low-energy sensors. The five-layer fiberglass/polyester composite laminated plate undergoes theoretical, numerical, and experimental examination for damage detection. Using piezoelectric wafer transducers (PZT) as actuators and sensors, experimental results validate theoretical findings. A strong agreement between experimental and numerical results, obtained through FEM using ABAQUS, is reported [10 & 11].

Three alternative actuation strategies are employed to drive flaps, altering vortex shedding from a nominally two-dimensional blunt trailing edge (BTE). Wind tunnel experiments, at a Reynolds number of 2600, reveal an increase in turbulent kinetic energy associated with two-dimensional vortex shedding from 70% to 90% when actuation frequency matches that of the natural wake process [12].

A magnetically connected piezoelectric harvester is examined, aiming to enhance responsiveness to broadband frequencies by adjusting the angular orientation of external magnets. Electromechanical equations incorporate multiple transverse magnetic force boundaries, empirically determined based on magnet angle, to describe nonlinear dynamic behavior. Notably, in cases of continuous acceleration exceeding the 0–25 Hz range [13 & 14].

Thin-film piezoelectric transformers are employed to generate Pico-level electricity through Carman Vortex Street. Using SOLIDWORKS software, a system of spiral streets capable of generating specific frequencies at defined water speeds is developed for simulation. The final prototype speed file of the nozzle is verified through testing, demonstrating increased speed over free current [15–18].

Wind energy harvesting can be used to power wireless sensors embedded in bridges, buildings, etc. One difficult issue is that the wind speed in some electronic environment is low, which leads to inefficient milled energy harvesting. This paper presents a novel nonlinear magnetic flap-based aerial energy harvester to enhance energy harvesting at low wind speeds. The presented harvester is mainly composed of a photoelectric beam, two 2D beams, and two external magnets [19-20].

Detecting and identifying damage to composite structures is an important part of monitoring and repairing structural systems in service to avoid immediate failure. Cost effectiveness and reliability are essential during the detection process. The Lamb wave method is an effective technique that is sensitive to small damages and can be applied to monitor structural integrity using low-power sensors. It can provide good information about the state of the structure during its operation by analyzing the wave propagation in the plate [21-22].

2. Materials and Method

a- The system

The piezoelectric patch is put under internal strain by the system's solid-cylindrical bluff body, which is coupled to a cantilever beam composed of 1060 aluminum because of its good elastic properties to induce internal strain on the piezoelectric patch. A substrate layer and a piezoelectric layer make up the cantilever beam. The piezoelectric is a double-layer product of piezo ceramic wafers (Piezo Protection Advantage PPA-2014). The cylinder is placed forward of the piezoelectric energy harvester, and both the cylinder and beam are immersed in the water. The water hit the cylinder to generate vortex shedding behind the cylinder. Vibrations are only carried out transversely. With consideration of the velocity of the water. The cantilever beam and cylinder are shown in figure (1a), and the dimensions and properties are listed in Tables 1 and 2. The harvester and circular cylinder are simulated in this study by using ANSYS WORKBENCH 2021 R2. First, the elements beam and piezoelectric were created by using SOLID45 and SOLID5, respectively. Second, the boundary condition is expended. SOLID45 contains 8 nodes, and there are 3 degrees of freedom (DOF) for each node. 3D solid constructions are represented using it. It has plasticity, creep, and stress stiffness swelling, large deflection, and large strain capabilities. SOLID5 comprises 8 nodes, and each node has 6 degrees of freedom. It has a restricted ability for coupling between fields and a 3D magnetic, piezoelectric, and structural field capacity.

In figure 1b, the computational domain is displayed. Its dimensions are 30 D for width and 20 D for depth. The domain is 10 D in length. The cylinder was placed at 10 D from the inlet boundary and in the symmetry of the other sides. The boundary conditions employed consisted of a velocity inlet on the right side and a pressure outlet on the left side, and all the walls were slipping on the duct.

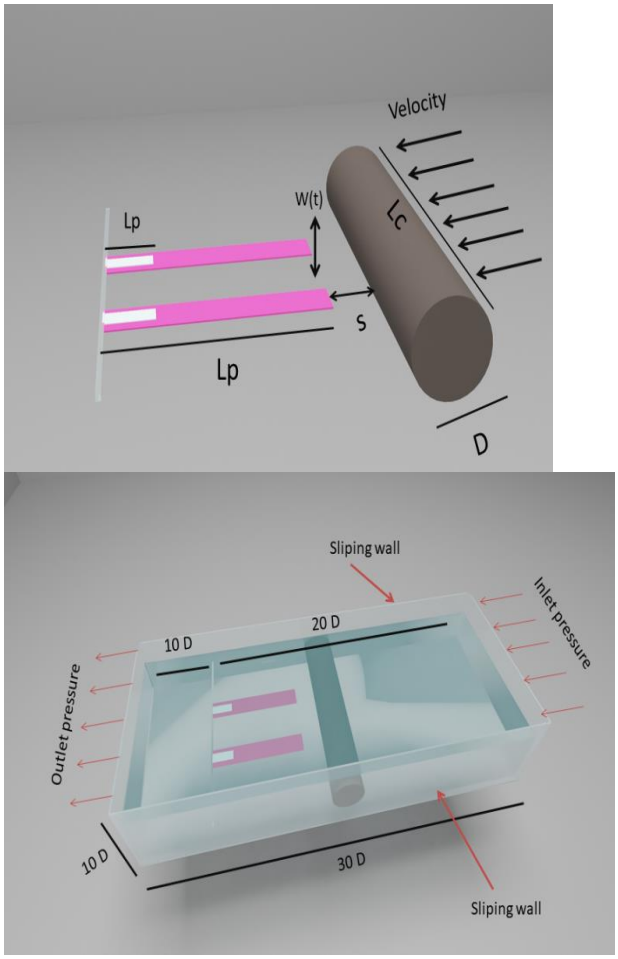

Figure (1): a- Schematics of the piezoelectric energy harvester under concurrent loading, b-Computation domains, and boundary conditions.

Table 1: Dimensions and Properties

Symbol	Description	Value	Units
$\rho_{cylinder}$	Circular Cylinder Oscillator Density	2700	Kg/m3
ρ_{fluid}	Fluid Density	997	Kg/m3
ρ_{beam}	Aluminum Beam Density	2700	Kg/m3
D	Cylinder Bluff-body Diameter	50	mm
$L_{cyl.}$	Length of the Cylinder	200	mm
L	Length of the Beam	300	mm
B	Width of the Beam	40	mm
h	The Thickness of the Beam	1.4	mm
L_p	Length of the Piezo	53	mm
B_p	Width of Piezo	20.4	mm
h_p	Thickness of Piezo	0.83	mm
E_b	Modulus of Elasticity of Aluminum	70E+9	Pa

υ	Poisson's ratio	0.34

Table (2): - The mechanical properties of piezoelectric (PZT) as the following.

Symbol	Description	Value	Units
d_{31} d_{33}	Piezoelectric Charge (displacem4e12ent) coefficient	Qar1	coul/N*10-12 or (m/v*10-12)
g_{31} g_{33}	piezo. voltage coefficient	19 -9.5	V.m/cm3
K_{31}	Piezoelectric coupling factor	0.38	
S_{11}^{E}	Piezoelectric compliance	$15.8 * 10^{-12}$	m^2/N
	Density	7350	kg/m^3
E	Modulus of Elasticity	68E+9	Pa
υ	Poisson's ratio	0.31	
	Material	PZH-5H	

b- Modeling

Research first determines the equation of the government system. The modeling equation relates the vibration of a bluff body (cylinder) to fluid flow. The equation also links these vibrations to the piezoelectric layer deformations in the cantilever beam. The energy that was extracted from the deformation of the piezoelectric layer is then computed. The modeling equation is established, and then ANSYS enhancements are researched. For this project, many design parameters have been found, and optimization has been done to identify the set of design parameters that collects the most power. To identify the best data that would optimize effort, a variety of distances between the cylinder and cantilever beam have been identified. The design parameters also include the cylinder's diameter, the fluid's velocity, and the beam's shape.

A set of parameter equations based on a set of design parameters regulate the ideal design parameters of the piezoelectric energy harvester to find optimal voltage and power, as stated in the preparation portion of this study. These equations are applicable to the piezoelectric energy harvesting system as intended.

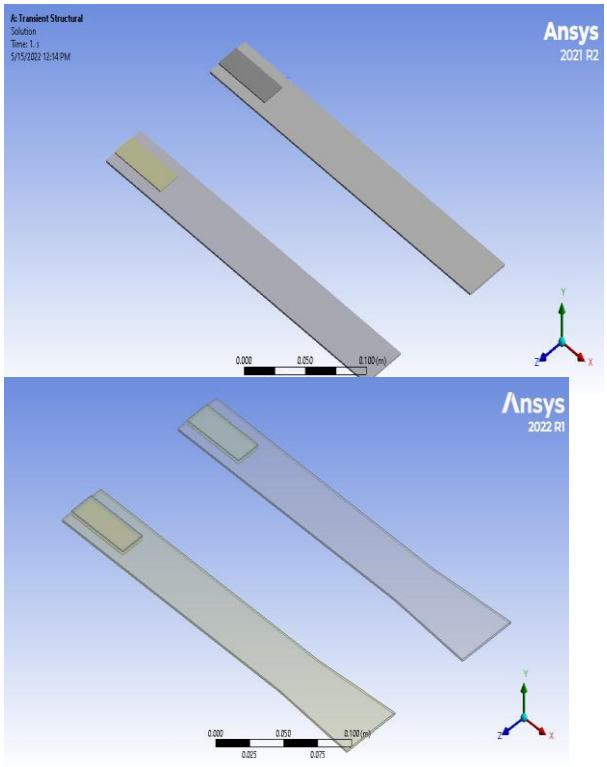

Figure (3): Finite element model for PEH.

c- Lifting Force Analysis

Our aim here is to create a linear force that vibrates. So, the electro-mechanical coupling can be increased. The confrontation and rationale of the optimized design of PEH are presented in this section.

Due to the nature of the vibrations resulting from the vortex shedding being irregular and nonlinear and the fact that there is no equation describing or controlling the lifting force that it exerted on the cylinder, the following equation has been extracted to describe the lifting force of the vortex induced vibration of the cylinder designed in this system to supply the greatest energy of the piezoelectric energy harvester.

To extract the equation of lifting force, the dimension-less analysis method was used, where the equation was obtained that correlates (material property) with (dynamic part), as well as the effect of the variables that have been studied and the effect of (vortex frequency of the system).

The lifting force is dependent on the geometry of the beam and flow parameters. Factors related to the geometry and dimensions of the test section, which can be summarized in Reynolds number (Re). The lifting force depend on the size of the cylinder (characterized by the diameter D in mm), the fluid velocity (V in m/s), the distance between bluff body (cylinder) and beam (S in mm), fluid and beam density (ρ and ρ_s respectively in kg/m^3), beam cross-section area and second moment of inertia (A_s and I in m^2 and m^4), the frequency (f in $1/s$), and young modulus (E in N/m^2).

The Buckingham π theorem and method of indices were used for finding dimensionless groups appropriate for this problem, and new empirical correlations were developed using the Multiple Linear Regression Method. The force exerted on the beam, it is assumed,

$$F = f(\rho_s, A_s, I, E, V, L, \rho, f, Re)$$

Where F is a function. This equation consists of nine variables with three basic primary dimensions needed to express the variables: distance [S] in mater, velocity [V] in meters per second, and diameter [D] in mater.

Based on the above, the number of dimensionless variables applicable to this problem was six.

By using a step-by-step approach, the six prime variables are selected, and another three repeated variables are found. The selected prime-dimensional variables are:

$$\rho_s \left[\frac{M}{L^3}\right], A_s\,[L^2], I\,[L^4], E\left[\frac{M}{L^2}\right], \rho\left[\frac{M}{L^3}\right], f\left[\frac{1}{T}\right] \qquad \ldots\ldots. (1)$$

The other repeated three-dimensional variables are:

$$L\,[L], V\left[\frac{L}{t}\right], D\,[L] \qquad \ldots\ldots.. (2)$$

The results of the dimensional analysis are in the following form:

$$F = (\pi_1, \pi_2, \pi_3, \pi_4, \pi_5, \pi_6) \quad \ldots\ldots\ldots (3)$$

$$\pi_1 = \rho\, V\, L\, F = \left(\frac{M}{L^3}\right)^a \left(\frac{L}{t}\right)^b (L)^c \frac{ML}{t^2} = M^0 L^0 t^0 = 1$$

$$M = a + 1 = 0 \rightarrow a = -1$$

$$L = -3a + b + c + 1 = 0 \rightarrow c = -2$$

$$t = -b - 2 = 0 \rightarrow b = -2$$

$$\pi_1 = \rho^{-1}\, V^{-2}\, L^{-2}\, F = \frac{F}{\rho\, V^2\, L^2} \qquad \ldots\ldots\ldots (4)$$

As per the same procedure, find the other π groups.

$$\pi_2 = \rho\, V\, L\, \rho_s \;\rightarrow\; \pi_2 = \frac{\rho_s}{\rho} \qquad \ldots\ldots (5)$$

$$\pi_3 = \rho\, V\, L A_s \;\rightarrow\; \pi_3 = \frac{A_s}{L^2} \qquad \ldots\ldots.. (6)$$

$$\pi_4 = \rho\, V\, L I \;\rightarrow\; \pi_4 = \frac{I}{L^4} \qquad \ldots\ldots. (7)$$

$$\pi_5 = \rho\, V\, L E \;\rightarrow\; \pi_5 = \rho V E \qquad \ldots.. (8)$$

$$\pi_6 = \rho\, V\, L f \;\rightarrow\; \pi_6 = \frac{L}{V} f \qquad \ldots\ldots (9)$$

$$\frac{F}{\rho\, V^2\, L^2} = f\left(\frac{\rho_s}{\rho}, \frac{A_s}{L^2}, \frac{I}{L^4}, \rho V E, \frac{L}{V} f, Re\right) \qquad \ldots\ldots. (10)$$

The groups on the right side can be reduced by multiplying some groups to produce one group, so the correlation becomes:

$$(mass)^0 (length)^0 (time)^0 = \left\{\left(\frac{\rho_s A}{EI}\right)^{1/2} VL\right\} * Re\left\{\frac{F}{1/2\rho V^2 A}\right\}\{f * t\} \quad \ldots\ldots. (11)$$

$$\frac{F}{1/2\rho V^2 A} = f\left(\left(\frac{\rho_s A}{EI}\right)^{1/2} VL, Re, ft\right) \qquad \ldots\ldots. (12)$$

A general formula for the lifting force can be set in the format

$$\frac{F}{\frac{1}{2}\rho V^2 A} = C\left[\left(\left(\frac{\rho_s A}{EI}\right)^{\frac{1}{2}} VL\right)^a, (Re)^b, (ft)^c\right] \qquad \ldots\ldots. (13)$$

where C, a, b, c are constants

Solving for the force under different conditions using the experimental data generated by the multiple linear regression method will give the following correlation:

$$\frac{F}{\frac{1}{2}\rho V^2 A} = 3.16 * 10^{-6}\left[\left(\left(\frac{\rho_S A}{EI}\right)^{\frac{1}{2}} VL\right)^{0.3} * (Re)^{0.734} * (ft)^{0.9}\right] \quad \ldots. (14)$$

$$F(t) = 1.58 * 10^{-6} * (\rho V^2 A)\left[\left(\left(\frac{\rho_S A}{EI}\right)^{\frac{1}{2}} VL\right)^{0.3} * (Re)^{0.734} * (ft)^{0.9}\right] \quad \ldots.. (15)$$

d- Mathematical Approach

Fluid forces can cause an excitation known as VIV, and the fluid-structure reaction must be studied. A system of block springs in the transverse direction can be used to characterize structural elasticity, as demonstrated in (2). This system may be simplified to have just one degree of freedom since the vortex vibration primarily occurs in the transverse direction (SDOF) [3]. Mathematical modeling, employing the second-order system known as "mass-spring-damper," as shown below, is one area of interest in the vibration behavior of the prototype.

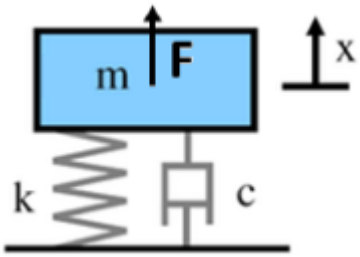

Figure (4):- A schematic of the proposed cylinder-based piezoelectric energy harvester.

$$M\ddot{y} + C\dot{y} + Ky = F_y(t) \quad \ldots.. (16)$$

Where M is the structural mass, c is the structural damping, k is the structural stiffness, x is the tip displacement in the harvester and $F_y(t)$ is the time-dependent transverse force acting on the model (the force by the vortex shedding on the cylinder) can be modeled as

$$\acute{F}(t) = 1.42 * 10^{-6} f * (\rho V^2 A)\left[\left(\left(\frac{\rho_S A}{EI}\right)^{\frac{1}{2}} VL\right)^{0.3} * (Re)^{0.734} * (ft)^{-0.1}\right] \quad \ldots.. (17)$$

This force is applied to the flexibly mounted cylinder using a stiffness spring to assemble K. The motion of the object described in the equation.

$$M\ddot{y} + 2m\zeta\omega_n\dot{y} + Ky = 1.58 * 10^{-6} * (\rho V^2 A)\left[\left(\left(\frac{\rho_S A}{EI}\right)^{\frac{1}{2}} VL\right)^{0.3} * (Re)^{0.734} * (ft)^{0.9}\right]..$$

(18)

ω_n is the natural frequency of the cylinder (rad/s), y is the vertical displacement of the cylinder, where the apostrophe represents a differential with respect to time, and ζ is a structural damping factor. For the linear oscillator model, the damping factor as a medium is estimated to be constant. This differential equation solves the equation for the linear displacement of the resulting cylinder with respect to time.

$$y(t) = \frac{F(t)}{k\sqrt{\left(1-\left(\frac{w_S}{w_n}\right)^2\right)^2 + (2\zeta\frac{w_S}{w_n})^2}} \quad \ldots.. (19)$$

In fact, the maximum capacity will occur in a frequency range rather than a precise resonance. However, the use of linear harmonic oscillator models provides an almost relatively accurate roller motion subject to VIV.

The linear harmonic oscillator model of VIV also allows the theoretical maximum energy to be calculated. Velocity as a cylinder time function can be obtained by distinguishing the displacement by the formula, resulting in the following equation:

$$v(t) = \frac{\dot{F}(t)}{k\sqrt{\left(1-\left(\frac{w_s}{w_n}\right)^2\right)^2+(2\zeta\frac{w_s}{w_n})^2}} \qquad \ldots\ldots (20)$$

Power as a function of time is found by multiplying the lift force and the cylinder velocity, which gives:

$$P = v(t) * F(t) \qquad \ldots\ldots. (21)$$

3. Experimental Work

The test sample to be used in the experimental work is two aluminum cantilever beams with two piezoelectrics, one on the top of the beam and the other on the bottom of each beam. The piezoelectric used in the energy harvester is a double-layer product PPA-2014 of 53*20.8*0.83 mm that has been fixed at the fixed end of the cantilever beam with epoxy glue. We used two shapes for the cantilever beam: one is the traditional beam, and the other is the optimized shape of the beam by adding a delta wing at the free end of the beam.

Piezoelectric transducers are based on the property of the electrical polarization of piezoelectric material under the action of a mechanical stress. In this case, the direct effect of piezoelectric materials will be investigated. The exploration of this technique aids in the enhancement of the system's total harvested electrical power. The design characteristics of the piezoelectric layers are depicted in Tables 1 and 2.

A material-class N42 block magnet has been fixed at the free end of the cantilever beam with epoxy glue. There are two anther magnets on the two sides of the cantilever beam, using the attraction force between two magnet sheets.

The system was put in duct with dimensions of 30D, 20D, and 10D as length, width, and height, respectively. Put the cylinder in front of the cantilever beam at a distance of 0.5 D and a cylinder diameter of 50mm. After that, it is tested with an optimal velocity of 1.25 m/s. These parameters are selected after testing, and if the optimal one is selected, the water will enter the duct and hit the cylinder to cause vortex shedding. Therefore, the vortex is used to vibrate the beam. The dimensions of the beam and piezoelectric are given in Table 3. The mechanical properties of aluminum 1060 are given in Table 4. The smart cantilever beam is shown in Figure 5. The experimental system is shown in Figure (6).

Table (3): Geometric Parameter of Beam and Piezoelectric

Geometric Parameter of Beam	Geometric Parameter of Piezo
$L = 300$ mm	$L = 53$ mm
$B = 40$ mm	$B = 20.4$ mm
$H = 1.4$ mm	$H = 0.83$ mm

Table (4): Mechanical Properties.

Properties	Aluminum
Young Modules	70 GPa
Density	2700 Kg/m3
Mass	variable

Poisson Ratio	0.34

Figure (5): the smart cantilever beam.

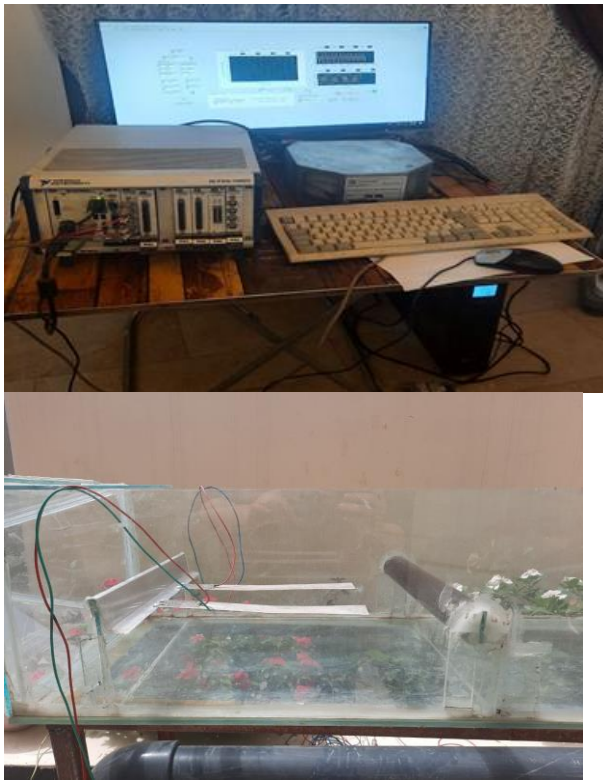

Figure (6): Experimental system.

The NIPXle 1062Q is used as an analog input to receive signals from piezoelectric. When a voltage is generated in Piezoelectric, NIPXle 1062Q simultaneously receives the output of the harvester signal as an analog signal and converts it into a digital signal for calibration and display in the LabView software. The program deals with the digital signal only. The harvester-controlled algorithms are embedded in the LabView software. Isolation transformers are used to isolate the system and provide electrical insulation as well as complete electrostatic insulation with noise insulation. A schematic view of the experimental system is shown in figure 7.

The computers that have data acquisition work as controllers in a real-time control application. The concordance of multiple data acquisitions is very important for sending and acquiring the data. The time step for data acquisition in an open-loop control system experiment is 0.001 s.

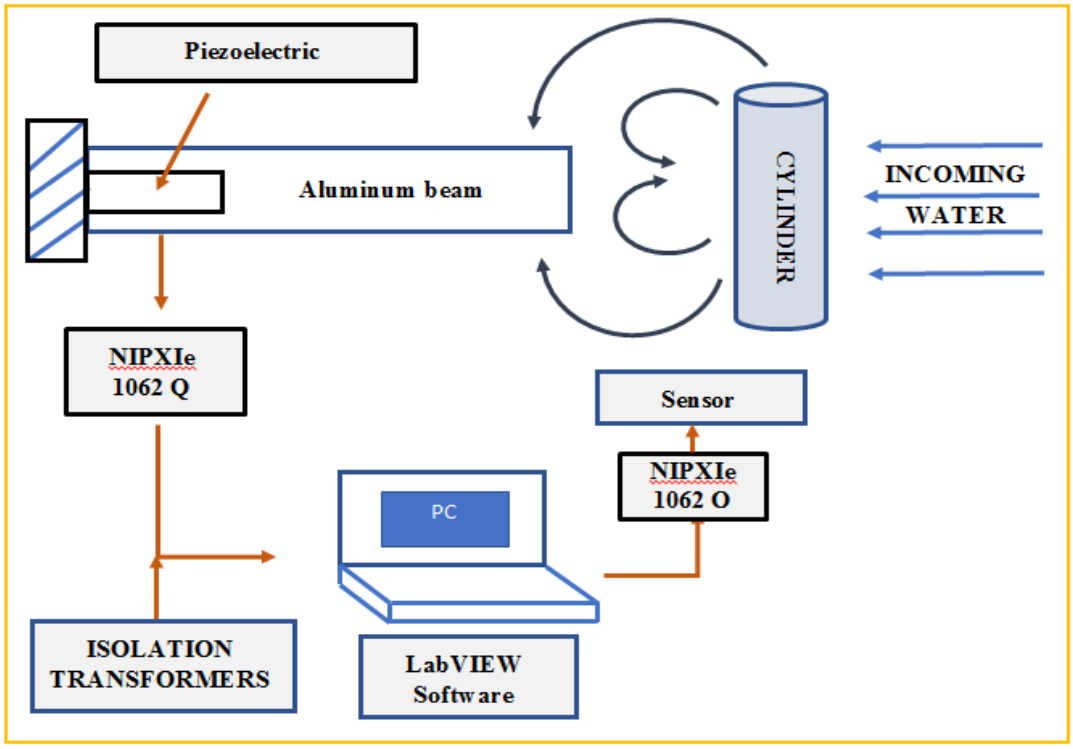

Figure (7): Schematic view of the experimental active vibration control setup.

4. Optimization Results

The force should be identified before looking at the coupling mechanism of the proposed piezoelectric energy harvester, PEH. A set of parameter designs is selected to optimize the PEH system. Using different locations between the bluff bodies (cylinder) and the beam (S), the fluid velocity (V) ranges between 0.5 and 2 m/s, the cylinder's diameter (D) ranges between 35 and 65mm, and the geometry of the cantilever beam is changed by adding a delta-wing to the free end. To understand the effect of a set of design parameters on the performance of PEH, the curves were simulated under different values of them.

a. Results of the Location of the Bluff Body

The following sites will be taken, and their impact on the overall performance of the harvester will be studied in this section. These sites are 3D, 2D, 1D, and 0.5D (where the D is the cylinder's diameter), and when studying the effect of these factors, we install the other factors. Where the following figure (8) shows the extent of the impact of the distance on the performance of the system. When selecting the first site, which is 3D, we see that there is no response to the system and no energy is generated under the influence of this site. After that, the site changes to 2D. We see that there is little response to the system, but this response did not generate energy from the harvester. After that, when using the third site, which is 1D, we see that the response is clear to the system, which resulted in the generation of energy from the harvester, but the generation was better when using the 0.5D site. The onset distance is 0.5 D.

At the end of this experiment, this factor was fixed at 0.5D because this site generates the best amount of energy for the harvester, and therefore, when conducting the rest of the experiments on other factors, only this site is used.

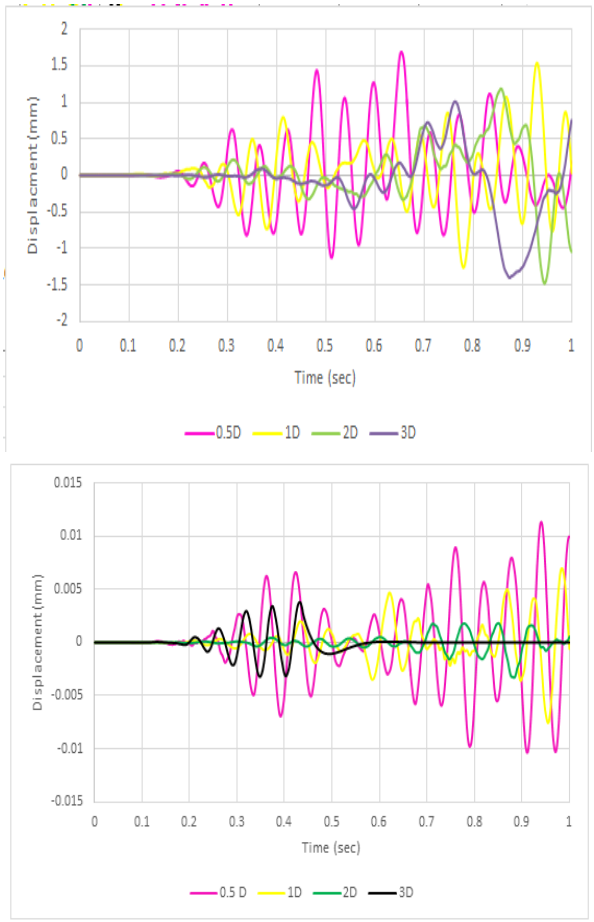

Figure (8): Vibration of the structure displacement with time for various distances, a) numerical result, b) experimental result.

b. Results of the Cylinder Diameter and Flow Velocity

Examine how the performance of the PEH system is affected by altering the diameter of the cylinder and the flow velocity in this section.

The vibration displacement perpendicular to the direction of the entering water is primarily responsible for the voltage generated by the piezoelectric cantilever beam. To ascertain the displacement waveform of the structure that varies over time, one may employ the central finite difference method. Water is entering at a rate of 0.75 to 2 m/s at V. The ideal velocity is 1.25 m/s, as can be observed by the maximum harvester power occurring at this velocity.

The vibration displacement's amplitude and frequency increase as water velocity increases, as shown in Figure 9. Additionally, it takes less time for the structure to sustain its oscillation cycle as the incoming water velocity increases. According to the wake angular frequency formula, the velocity of the entering water is precisely proportional to the frequency of the fluid. The energy harvester's damping and stiffness terms and wake frequency are connected. It results in a rise in frequency and displacement amplitude with the increase of

To further bolster the theoretical mathematics and solution model of the piezoelectric harvester underwater, an experimental study is carried out, with the results shown in Figure 10.

The cylinder diameter D is varied between 35mm and 65mm with a step of 15mm. According to the figures (11 and 12), the optimum diameter is 50mm due to the maximum harvester power generated.

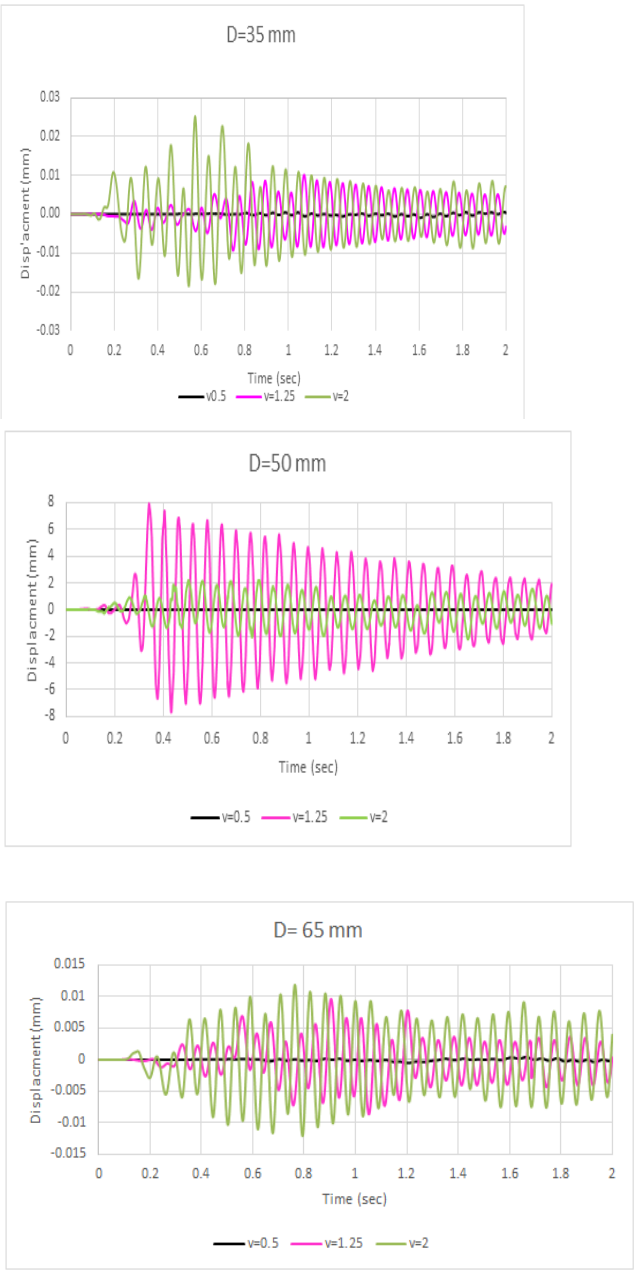

Figure (9): Vibration of the structure displacement with time for various incoming water velocities, numerical results.

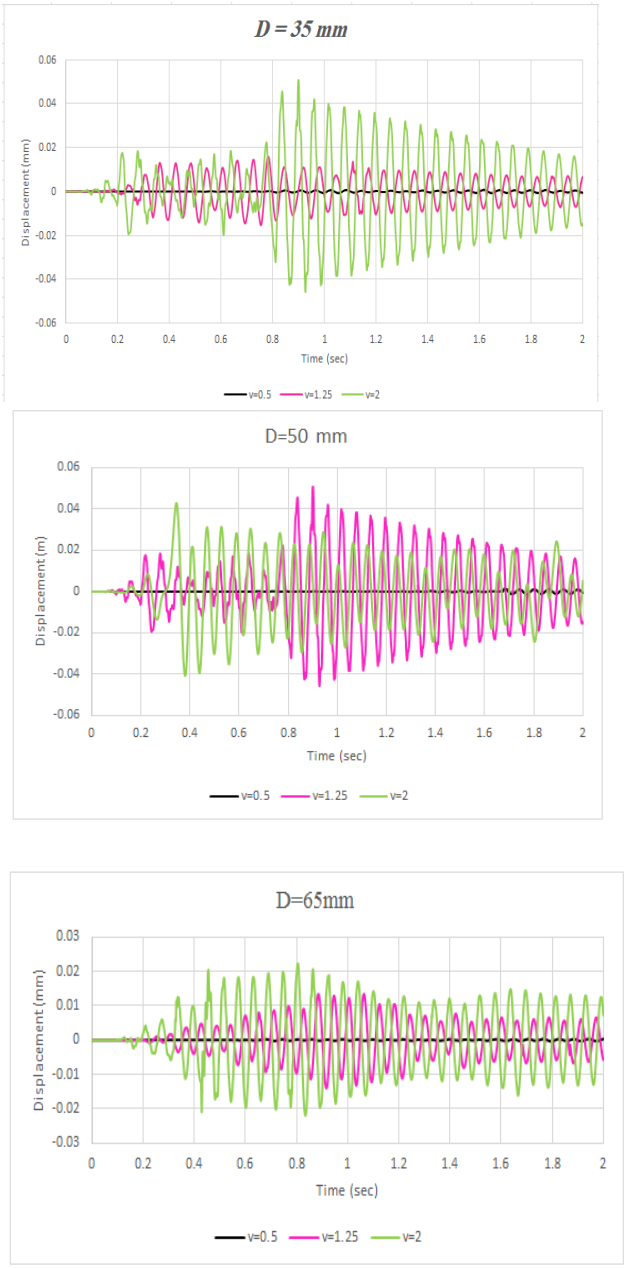

Figure (10): Vibration of the structure displacement with time for various incoming water velocities, experimental results.

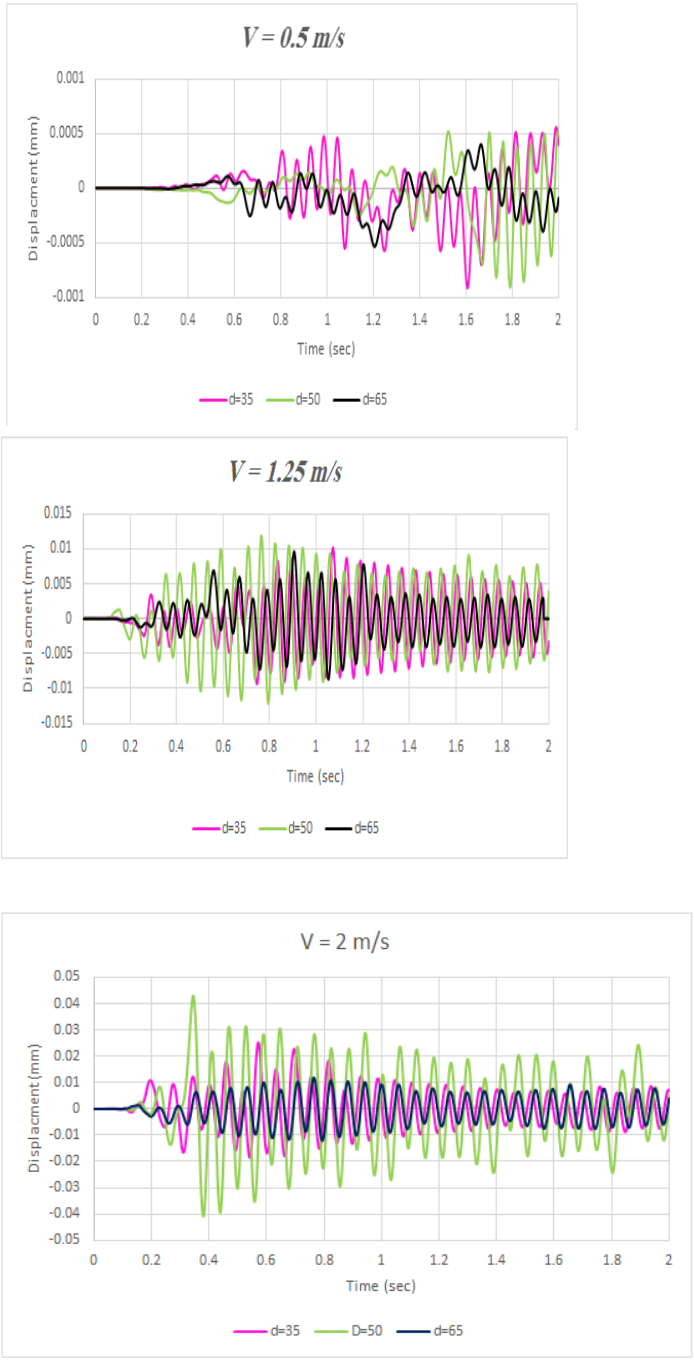

Figure (11): Vibration of the structure displacement with time for various incoming water velocities, numerical results.

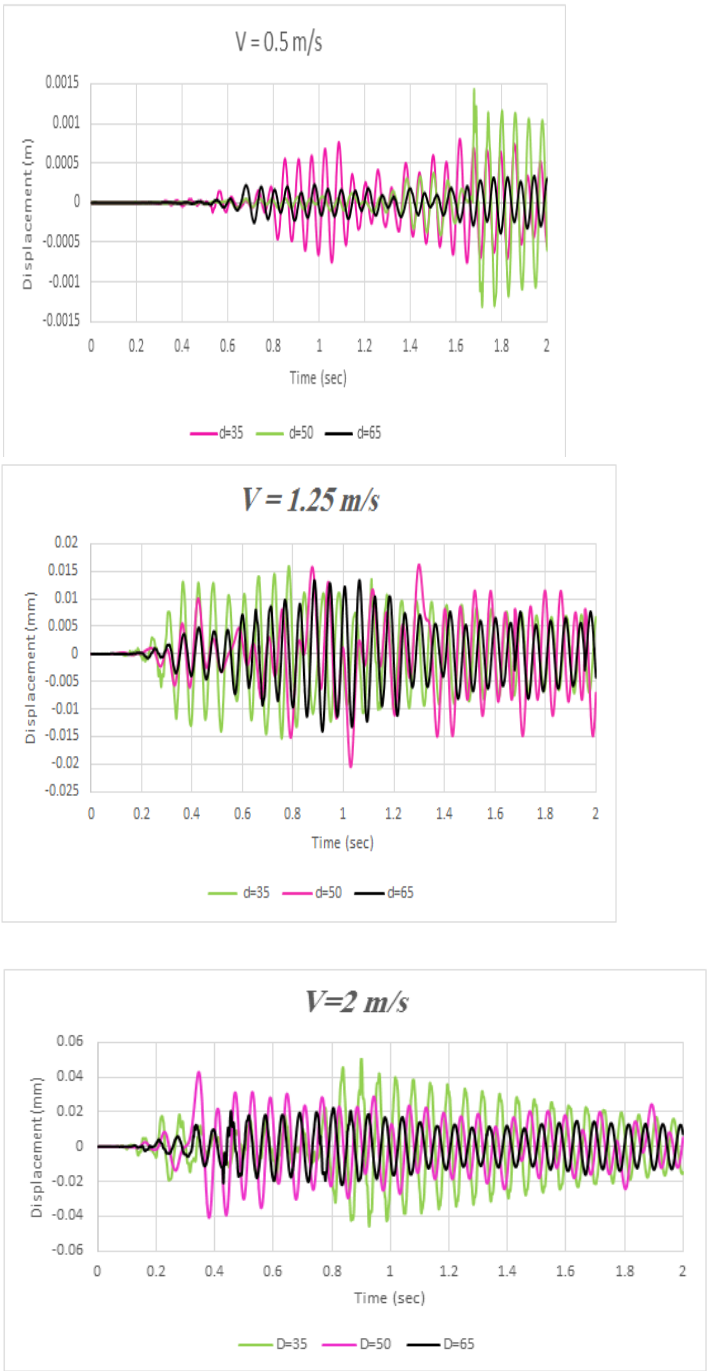

Figure (12): Vibration of the structure displacement with time for various incoming water velocities, experimental results.

To learn more about the structural vibration response, fast Fourier transform (FFT) analysis may be used to determine the oscillation frequency. The frequency spectrum is depicted in Figure 13 for water velocities of 0.5 m/s, 1.25 m/s, and 2 m/s, respectively. It is evident that each frequency spectrum has a displacement peak at 0 Hz that is caused by the specified stimulating force.

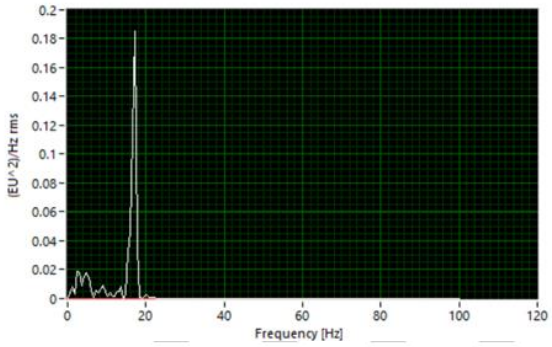
(EU^2)/Hz rms
Frequency [Hz]

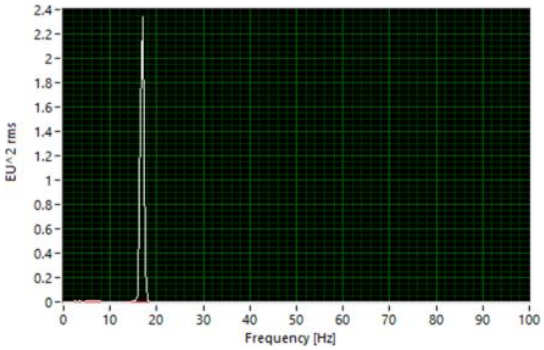
EU^2 rms
Frequency [Hz]

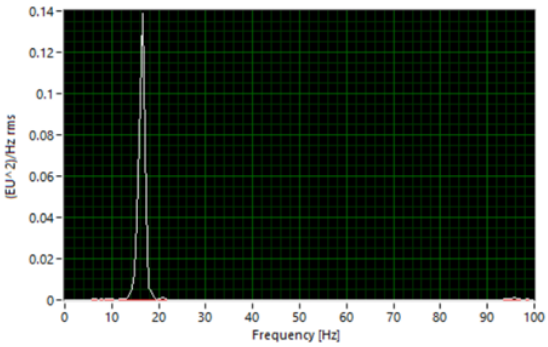
(EU^2)/Hz rms
Frequency [Hz]

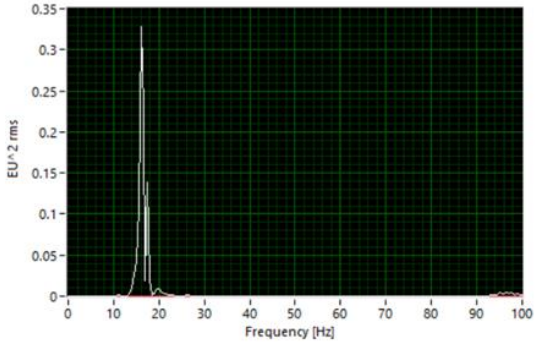
EU^2 rms
Frequency [Hz]

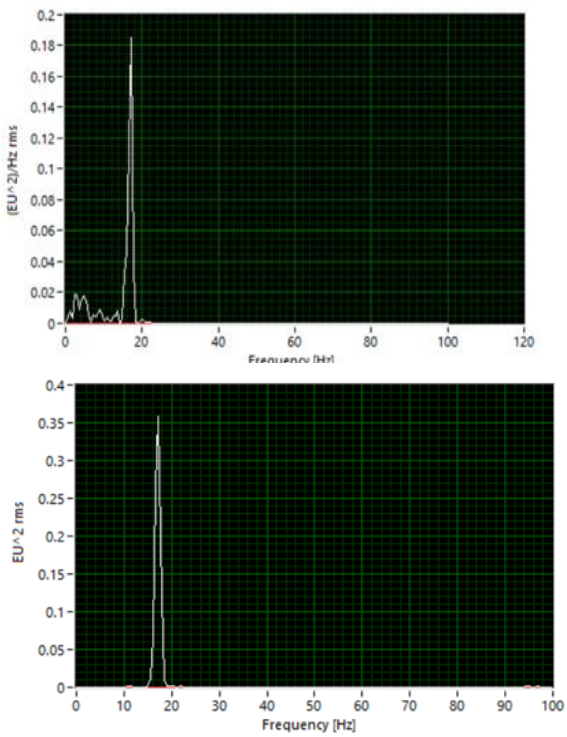

Figure (13): Fast Fourier Transform analysis with the velocity of (a) 0.5 m/s, (b) 1.25m/s, (c) 2 m/s, and diameter (d) 35mm, (e) 50mm, (f) 65mm.

c. The Results of the Geometer of the Beam

In this section, study the effect of changing the geometry of the beam on the performance of the PEH system.

By adjusting the piezoelectric cantilever's design and material, which will also have an effect on its strength condition, the PEH yield may be raised. This study implements the step, which suggests a delta-wing structure to further enhance the output, in order to boost PEH production.

The geometry of the cantilever beam changes from a traditional beam to an optimal shape by adding a delta-wing to make the width of the beam 40mm at the fixed end and 50mm at the free end. There is an optimization in the generated power of the harvester, as shown below.

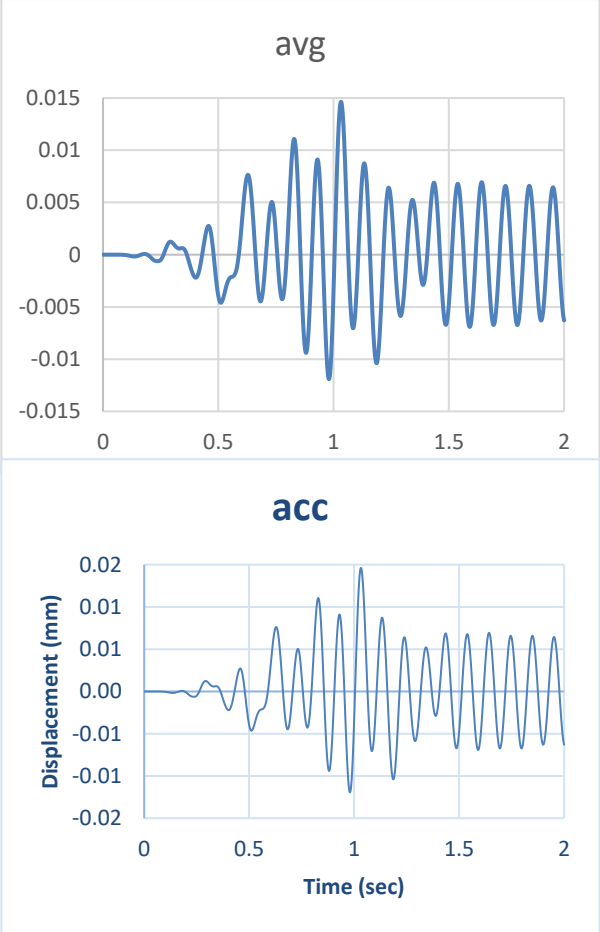

Figure (14): Vibration of the structure displacement with time for optimized shape, a) numerical results, b) experimental results.

5. Conclusion

The design optimization of a hydropower harvesting system was thoroughly examined in this study, considering various parameters. Depending on the prevailing flow conditions, the model's variables can be readily adjusted, leading to a rationalized optimal design. As expected, the lift force generated is markedly influenced by the interplay of factors including the bluff body's location, cylinder dimensions, and flow velocity. From these findings, empirical equations correlating the lifting force and displacement, derived from the force equation, were established.

Numerous energy harvesting methodologies hinge on the reciprocating motion inherent in the involved structural system. The methodology developed in this study has demonstrated its effectiveness in yielding optimal designs for such energy harvesting devices, provided that the stipulated assumptions and constraints detailed in this paper are met.

The design process commences with the formulation of modeling equations, which are functions of four critical design parameters. Executed within ANSYS, this model produces an optimized system configuration. Consequently, the values representing the generated power for these optimal design parameters are determined.

Through the exploration of various design factors, the most favorable outcomes were attained with a distance of 0.5 D between the beam and the cylinder, a cylinder diameter of 50 mm, and a flow velocity of 1.25 meters per second.

References

[1] Morgan Funderburk & Yujin Park & Anton Netchaev& Kenneth J. Loh, 2022, Piezoelectric Rod Sensors for Scour Detection and Vortex-induced Vibration Monitoring, University of California.

[2] Sondipon Adhikari & Arnab Banerjee, 2021, Enhanced low-frequency vibration energy harvesting with inertial amplifiers, Article in Journal of Intelligent Material Systems and Structures.DOI:10.1177/1045389X211032281.

[3] E van de Wetering & T W A Blad & R A J van Ostayen, 2021, A stiffness compensated piezoelectric energy harvester for low-frequency excitation, Smart Materials and Structures, 30 (2021) 115001 (11pp).

[4] Christina Hamdan & John Allport & Azadeh Sajedin,2021, Piezoelectric Power Generation from the Vortex-Induced Vibrations of a Semi-Cylinder Exposed to Water Flow, Basel, Switzerland.

[5] Quan Wang & Kyung-Bum Kim & Sang-Bum Woo & Yooseob Song & Tae-Hyun Sung, 2021, A Magneto-Mechanical Piezoelectric Energy HarvesterDesigned to Scavenge AC Magnetic Field from Thermal PowerPlant with Power-Line Cables. Energies MDPI.

[6] Hayder F.N. Al-Shuka, 2020, Proxy-Based Sliding Mode Vibration Control with an Adaptive Approximation Compensator for Euler-Bernoulli Smart Beams, Journal Européen des Systèmes Automatisés Vol. 53, No. 6, December, 2020, pp. 825-834.

[7] Min Liu & Hui Xia & Guoqiang Liu,2021, Experimental and numerical study of underwater piezoelectric generator based on Vortex-induced Vibration, School of Electronic Electrical and Communication Engineering, University of Chinese Academy of Sciences, Beijing, 100190, People's Republic of China.

[8] Yin Jen Lee & Yi Qi1, Guangya Zhou & Kim Boon Lua,2019, Vortex-induced vibration wind energy harvesting by piezoelectric MEMS device in formation, Singapore Academic Research Fund (AcRF) FRC Tier 1 Grant (R-265-000-585-114).

[9] Hani Kamal Chyad Khalil & Nabil Hassan Hadi,2019, Non-Destructive Damage Assessment of Five Layers Fiber Glass / Polyester Composite Materials Laminated Plate by Using Lamb Waves Simulation, College of Engineering–University of Baghdad,Number 5 Volume 25.

[10] Bradley Gibeau, Charles Robert Koch, and Sina Ghaemi, 2019, Active control of vortex shedding from a blunt trailing edge using oscillating piezoelectric flaps, American Physical Society, PHYSICAL REVIEW FLUIDS 4, 054704

[11] Bradley Gibeau & Charles Robert Koch & Sina Ghaemi, 2019, Active control of vortex shedding from a blunt trailing edge using oscillating piezoelectric flaps, Department of Mechanical Engineering, University of Alberta, Edmonton, Alberta T6G 2R3, Canada.

[12] Shengxi Zhou & Junyi Cao & Alper Erturk & Jing Lin, 2013, Enhanced broadband piezoelectric energy harvesting using rotatable magnets, State Key Laboratory for Manufacturing Systems Engineering, School of Mechanical Engineering, Xi'an Jiaotong University, Xi'an 710049, China.

[13] c. Jimenez-Gonzalez & F.J. Huera-Huarte, 2018, Vortex-induced vibrations of a circular cylinder with a pair of control rods of different sizes, Journal of Sound and Vibration .

[14] James Doty, Christopher Mayforth, and Nicholas Pratt, 2018, Karman Vortex Street Energy Harvester for Picoscale Applications, WORCESTER POLYTECHNIC INSTITUTE.

[15] Natalie Diltz & Julie Gagnon & Jacqueline O'Connor Jessica Wedell, 2017, Vortex Induced Vibration Energy Harvesting through Piezoelectric Transducers.

[16] Takeshi Ishihara & Tian Li, 2020, Numerical study on suppression of vortex-induced vibration of circular cylinder by helical wires, Department of Civil Engineering, School of Engineering, The University of Tokyo, Tokyo, 113-8656, Japan.

[17] Wanhai Xu & Wenqi Qin & Xifeng Gao, 2018, Experimental Study on Streamwise Vortex-Induced Vibration of a Flexible, Slender Cylinder, State Key Laboratory of Hydraulic Engineering Simulation and Safety, Tianjin University, Tianjin 300072, China.

[18] Yiannis Constantinides & Owen H. Oakley, Jr, 2006, Numerical Prediction Of Bare And Straked Cylinder Viv, 25th International Conference On Offshore Mechanics And Arctic Engineering,Hamburg, Germany.

[19] Kui Li Zhichun Yang Yanga & Yingsong Gu & Shun He & Shengxi Zhou, 2018, Nonlinear magnetic coupled flutter based aeroelastic energy harvester: M odeling , simulation and experimental verification, School of Aeronautics, Northwestern Polytechnical University, Xi'an 710072, China.

[20] Sondipon Adhikari & Akshat Rastogi & Bishakh Bhattacharya, 2019, Piezoelectric vortex induced vibration energy harvesting in a random flow field.

[21] Hayder F N Al-Shuka & Kareem Jawad Kadhim & AbdnoorJameel Shaheed Alhamadani, 2021, On modelling and adaptive control of a linear smart beam model interacting with fluid, IOP Conf. Series: Materials Science and Engineering.

[22] Hani Kamal Chyad Khalil and Nabil Hassan Hadi, 2019, Non-Destructive Damage Assessment of Five Layers Fiber Glass / Polyester Composite Materials Laminated Plate by Using Lamb Waves Simulation, Journal of Engineering journal homepage: www.joe.uobaghdad.edu.iq Number 5 Volume 25 May.